Spring 2015

Characterizing the influence of carbon on the flowrate and disinfection efficacy of household ceramic water filters

Jessie Yvonne Hahn

Department:

CHARACTERIZING THE INFLUENCE OF CARBON ON THE FLOWRATE AND DISINFECTION EFFICACY OF HOUSEHOLD CERAMIC WATER FILTERS

by

JESSIE YVONNE HAHN

A THESIS

Presented to the Faculty of the Graduate School of the

MISSOURI UNIVERSITY OF SCIENCE AND TECHNOLOGY

In Partial Fulfillment of the Requirements for the Degree

MASTER OF SCIENCE IN GEOLOGICAL ENGINEERING

2015

Approved By

Dr. A. Curt Elmore

Dr. Norbert Maerz

Dr. Mary Reidmeyer

PUBLICATION THESIS OPTION

This thesis includes an article prepared for submission to the journal *Water Science and Technology: Water Supply*. The content of pages 14-30 will be submitted for publication in that journal. Please note that sections of this document contain additional information supplemental to the journal paper.

ABSTRACT

Drinking water contamination is a major cause of disease in developing countries. Point of Use (POU) water treatment technologies generally have low initial cost and allow rapid availability of improved water. Ceramic pot filters (CPFs) are a POU water source treatment technology which filter water by gravity through a porous ceramic media. Some filters in use contain carbon remnants left from the fugitive pore former as a dark carbon core. Using disk-shaped experimental ceramic filters produced in the lab to have varying levels of carbon, the percent carbon present was measured and a visual analysis method was developed to determine a representative carbon content statistic for the filters. A semi-logarithmic relationship was found between the physical carbon analysis method and the visual carbon analysis method. This visual analysis methodology could be used by CPF production centers to quickly evaluate the carbon content in production CPFs. Sawdust used as a pore former has been noted as a potential source of flowrate variability. The sawdust used in this study was analyzed from digital imagery for shape and size variation and was found to have a high degree of variability. The experimental filters were installed in reactors and contaminated water was run through them over the course of four weeks. Flowrate and logarithmic reduction values (LRV) were determined for each filter at the end of the four weeks. No direct benefit was identified for the presence or the absence of carbon, however, a marginal benefit of complete burnout of carbon is a more focused grouping of flowrate and LRV. Since flowrate is a common quality control test, the smaller variability in flowrate and LRV could contribute to a more efficient manufacturing process with fewer rejected filters and a more consistent final product.

ACKNOWLEDGMENTS

I would like to thank my advisor, Dr. Curt Elmore, for sharing his extensive experiences and abounding knowledge to assist my research endeavors. His guidance has been imperative throughout my experience at Missouri S&T.

I would also like to thank my committee members, Dr. Mary Reidmeyer and Dr. Norbert Maerz, for their interest in this project and for their assistance. I would like to especially thank Dr. Reidmeyer for her extensive help in the production of appropriate experimental filters for the study, and Dr. Maerz for sharing his knowledge of image processing.

I would also like to thank the CPF factory near Antigua, Guatemala for the opportunity to observe their process and learn about the filters, and for the inspiration to investigate the carbon remnants.

I would also like to thank my office mates, Dr. Yovanna Cortes Di Lena, Carlo Salvinelli, and Kayla Speidel for their encouragement and support. I also want to thank my family for their continued support throughout my education and Tommy Goodwin, Jr. for his assistance in research and in stressful times.

TABLE OF CONTENTS

Page

LIST OF ILLUSTRATIONS

LIST OF TABLES

LIST OF ABBREVIATIONS

CPF	Ceramic Pot Filter
CV	Coefficient of Variation
LRV	Logarithmic Reduction Value
POU	Point Of Use

1. INTRODUCTION

1.1 BACKGROUND

According to the World Health Organization and the United Nations Children's Fund (WHO and UNICEF, 2014), 748 million people did not have access to improved drinking water sources in 2012. Improved drinking water sources can be a centralized system for a community or a point of use (POU) system designed to provide water for one household. POU treatment systems are an effective option in rural communities without a central improved water source because POU technologies require less infrastructure and initial expenditure, making the improved water available to the household sooner (Sobsey et al., 2008). One effective POU technology is the ceramic pot filter (CPF) (Hunter, 2009). CPFs are porous ceramic filters with a tapered cylindrical pot shape applied with colloidal silver or silver salt as a disinfectant. As seen in Figure 1.1, water, poured into the pot-shaped filter, flows by gravity through the CPF and into a plastic bucket to be dispensed via a spigot for drinking.

Figure 1.1: Typical CPF. A lid is placed on top to exclude additional contamination.

1.2 MOTIVATION

1.2.1 Influence of Carbon Content. The authors had the opportunity to work with a factory that produces CPFs near Antigua, Guatemala where carbon remnants of the pore former remain in the final production product, as seen in Figure 1.2. The CPF factory describes the carbon remnants as activated carbon that should add to the removal of bacteria and improving the taste of the water. However, the Ceramics Manufacturing Working Group (2011) notes that additional research is needed to explore the influence of the carbon core on the efficacy and lifetime of the CPFs and recommends complete burnout for the most effective filters. This study investigates the carbon remnants in the CPFs, focusing on the influence of varying levels of carbon remnants in the filters on short-term filter efficacy and flowrate as well as building a tool to visually evaluate the relative carbon content in a CPF.

Figure 1.2: Carbon remnants in CPF cross sections.

1.2.2 Visual Carbon Content. Analysis of carbon performed for this study was done by laboratory analysis, which requires time and money to achieve. A visual analysis

method was developed to determine a general carbon content more quickly and economically than a laboratory analysis.

1.2.3 Pore Former Variability. Hubbel et al. (in press) has hypothesized that the variability in flowrate observed in her study may have been caused by the variability in the pore former (sawdust). The sawdust used in this study was analyzed through microscopy for size and shape variation.

2. OBJECTIVES

2.1 PROBLEM STATEMENT

The presence of residual carbon in CPFs has been observed at a factory in Guatemala as a result of incomplete burnout of pore former. The practice of incomplete burnout is not recommended by the Ceramics Manufacturing Working Group (2011), which also noted that the effects of the carbon in the pores have not yet been studied. The

2.2 STUDY OBJECTIVES

The objectives of this research were to:

- Observe the CPF production process at a factory near Antigua, Guatemala where filters are produced with carbon remnant inclusions
- Produce experimental filters that emulated filters produced in the CPF factory
- Analyze the carbon content in the experimental filters
- Develop a method to determine carbon content through visual analysis
- Determine flowrate and LRV for the experimental filters
- Analyze variability in pore former material (sawdust)
- Analyze the relationship between carbon content and flowrate
- Analyze the relationship between carbon content and LRV

3. METHODS

3.1 OBSERVED FILTER PRODUCTION PROCESS

The authors observed the CPF manufacturing process at a factory near Antigua, Guatemala. The raw materials used are clay, sawdust, and water. The sawdust, which is passed through a wire mesh to eliminate particles larger than a No. 8 sieve, acts as a fugitive pore former to increase porosity and permeability. Clay from Rabinal, Guatemala is mixed with the sieved sawdust at an approximate weight ratio of 6:1 clay-to-sawdust and wetted to create a working body. When it appears homogenous, the working body passes through an extruder to finalize mixing. The working body is then formed into a pot shape with a mechanical press, as seen in Figure 3.1. The shaped CPFs are then set to dry completely on shelving in the open-air factory for 1 to 3 weeks before being fired in a propane-fired kiln in batches of approximately 200. The fired filters are soaked in water overnight to saturate prior to a quality control flowrate test. A one-hour falling head test is conducted in duplicate to ensure that the flowrates of the filters are between 1 and 2 litres per hour. Filters that pass the flowrate test are painted inside and out with colloidal silver in solution.

Figure 3.1: Shaping a CPF with a mechanical press.

The firing schedule used by the factory near Antigua, Guatemala leads to the presence of a black core of incompletely combusted sawdust (carbon) remaining in the filters. The firing process has a total duration of 7 to 8 hours. Two hundred filters are fired in a kiln during one firing. The factory has two kilns, each with six burners. The kiln burners are operated for three hours to raise the temperature to 450 to 500^{o}C. The sawdust in the filters has ignited by the time this temperature is reached, and the burning sawdust causes the temperature to begin to increase more quickly. The burner is then turned off for 1.5 hours with the vents closed, as seen in Figure 3.2, which limits the oxygen in the kiln. The limited oxygen smothers the flames and induces a reducing (oxygen-limited) atmosphere. The reducing atmosphere will allow the kiln to increase in temperature at a slower, more consistent rate, which is necessary to keep the filters from cracking. After the 1.5 hours with the vents closed, the burners are turned on again, increasing the temperature

Figure 3.2: Closing the vents on the kiln.

to a maximum of 750ºC before the kiln is turned off and the top vents are opened for cooling. The open vents allow some burnout of carbon beginning from the outside of the CPFs; however, oxygen is limited and the burnout occurs slowly. Once the kiln temperature cools below the combustion point of the sawdust the burnout stops, leaving a carbon remnant core in the CPFs.

3.2 EXPERIMENTAL FILTER PRODUCTION PROCESS

The filters used in this study were manufactured on the Missouri University of Science and Technology campus from a synthetic clay body with a process that attempted to simulate the production process in the factory near Antigua, Guatemala. The clay body used was developed in an earlier study to resemble the clay from Rabinal, Guatemala used in the CPF factory (Hubbel et al., in press). Lower levels of iron in the clay developed by Hubbel et al. (in press) gave it a lighter color relative to the native clay from Rabinal which was determined preferable as the lighter color would make the dark carbon core more apparent for visual analysis. The sawdust used, a red oak sawdust obtained from Dr. Huebner's woodworking shop, was passed through a No. 8 sieve, combined in a 6:1 weight ratio with the clay, and mixed with deionized water until homogenous. The filter shape chosen for this study is a disk shape, similar to that used by Oyandel-Craver and Smith (2007) and Ren and Smith (2013). Thirty disks were formed with a circular manual press set to the thickness of the bottom of the filters produced in Guatemala. The resulting disk-shaped filters had a diameter of 10 cm and a thickness of 2 cm. After pressing and before firing, the filters were allowed to dry for at least a week and spent at least 8 hours drying in a soils oven set at 100ºC. The filters in this study were not applied with colloidal silver

in an effort to simplify the focus of the study because CPFs have been found effective even without silver present (Oyandel-Craver and Smith, 2007; Clark and Elmore 2011).

The filters were fired in an electric kiln in three separate firings with different atmospheres. The firing schedule (temperatures and times) was the same for each of the firings, but the atmosphere was different for each firing. The firing schedule slowly increased the kiln temperature to 993^{o}C over the course of 14 hours before allowing it to cool back to room temperature. The same firing schedule was used in Hubbel et al. (in press) when she developed the clay body used in this study. Ten filters were fired in each firing. For the mid-range atmosphere firing, oxygen was limited locally by placing the filters in a cordierite sagger box with a partial seal, and placing other combustible material (additional sawdust) in the sagger box to partially scavenge oxygen that entered the box. The resulting atmosphere limited oxygen to result in incomplete burn out and leave some carbon remnants. Filters that were closer to an oxygen source (nearer to the top of the box) experienced greater burnout than filters farther from an oxygen source (nearer to the bottom of the box), leading to greater variation in carbon in the mid-range firing. For the reducing atmosphere firing, the process was repeated with additional combustible material in the cordierite sagger box and a thicker, more complete seal. The filters in this firing experienced less burnout than the first firing with more carbon remnants left in place. The oxidizing atmosphere firing was performed in air (without a sealed box), causing all of the sawdust to fully combust.

After firing, the filters that had incomplete combustion had more carbon remnants in the central region than around the edges because the oxygen was able to penetrate into the edges more than into the center. To obtain a more homogenous disk for testing, a

smaller disk 5 cm in diameter was cut from the center of each disk. Figure 3.3 illustrates the removal of the disk and which portions of the fired filter were used for testing.

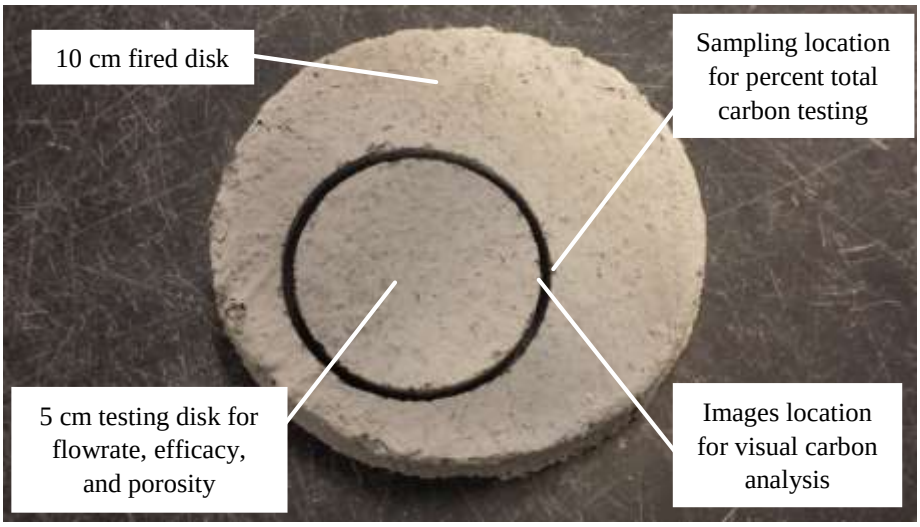

Figure 3.3: Diagram of filter for testing.

3.3 ANALYSIS OF FILTERS

The content of carbon was analyzed both visually and physically. The physical investigation was performed by powdering approximately 5 grams of the inner perimeter of the 10 cm disks from which the 5 cm disks were removed (see Figure 3.3). The powder was then sent to the University of Missouri Extension Soil Testing Laboratory in Columbia, Missouri for total carbon analysis. The percent total carbon analysis was performed by combustion method using an Elementar Vario MAX Carbon/Nitrogen Analyzer.

Visual testing was performed by taking 3 images along the circumference of the filter disks with both a Leica S8APO digital stereoscope and a HiROX KH-8700 digital microscope. The two instruments were used in order to have two different image sets of the same physical filters so that they could be compared to validate the developed visual

methodology. The images taken with each digital imaging device used the same shutter speed, light settings, and image parameters. Each image was cropped to include only the filter material and then converted to greyscale. Matlab code was written to import the images as an array with a value (0 for black to 255 for white) for each pixel of the image, then to return the median value of the array to get a representative tone value for the image. The values were averaged for the three images of each filter to obtain a representative tone for that filter. Appendix H includes a few representative images in print and all images used in this study on a CD-ROM.

Shards from production filters made at the factory in Guatemala were also visually analyzed for carbon content to show that they contain carbon and that they contain variable amounts of carbon. These CPFs were observed to have a carbon core in the interior and full burnout at the surface. Three images were taken from the surface of the CPF shard to be representative of a filter that had experienced full burnout. Seven images were taken of a cross-section of the filters to show the carbon core. These images were taken on both the Leica stereoscope and the HiROX microscope, and were processed in the same way as the experimental filter images to produce a representative value for each image. A paper standard was used to identify differences between the Leica stereoscope and the HiROX microscope images. The standard consisted of six printed blocks of color: white, white darker 5 percent, white darker 15 percent, white darker 50 percent, black lighter 25 percent, and black. An image was taken of each color block on each imaging device. These images were processed in the same way as the production filter images and the experimental filter images to identify a representative tone value for each image.

The porosity of the filters was determined in order to find the pore volume for the filters. A modified Archimedes method (ASTM C830-00) was used to characterize the apparent porosity of two experimental filters, one with complete burnout and one with incomplete burnout (with apparent high carbon content), in order to determine a general difference in the porosity values between high carbon filters and low carbon filters. Instead of using a vacuum and pressure chamber to saturate the samples, each sample was left to soak submerged in water for at least 18 hours to achieve saturation. This procedure is similar to the procedure followed by the CPF factory in Guatemala to saturate their filters before flowrate testing. This modified saturation procedure may not fully saturate the small pores in the clay body, but the clay body porosity was assumed to be small compared to the porosity caused by the pore former.

Six filters from each firing were affixed inside plastic tubes, for a total of 18 experimental reactors, as seen in Figure 3.3. The filters were disinfected to insure that they had not been contaminated after firing. Disinfection was performed according to the procedure used by Clark and Elmore (2011) with three pore volumes (45 mL total) of bleach water solution (0.08 mL/L chlorine). Once the filters were disinfected, each filter was filled with a sodium thiosulfate solution (0.25 mg/L) to remove any residual chlorine. The effluent water was tested for total chlorine with a Hach Total Chlorine field kit (CN-66T) to ensure that all chlorine was removed. If the test came back with any presence value for total chlorine, additional sodium thiosulfate solution was passed through the filter to eliminate the chlorine until the Total Chlorine low range test was below the detection limit. A presence/absence Colilert® coliform test analyzed the effluent from each filter to ensure that there were no coliforms present in the effluent from the filters before testing began.

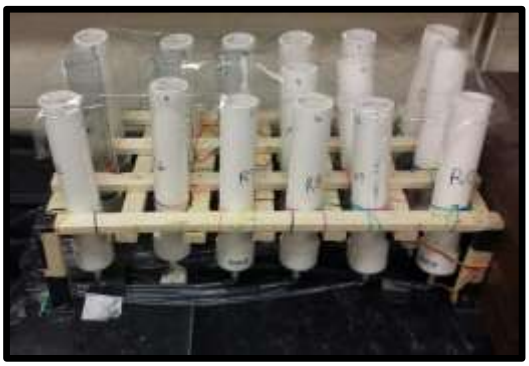

Figure 3.4: Experimental setup for flowrate and LRV testing.

To test the filters, a simulated contaminated surfaced water was produced using influent from the wastewater treatment plant (WWTP) in Rolla, Missouri and passed through the filters for four weeks. The filters were filled to 23 cm of water, which is the same head as a filled production CPF would experience. The WWTP influent was mixed with tap water to create the testing influent water ("challenge" water) for the filters, which was passed through the filters for four weeks. The challenge water was on the order of 10^2 colony forming units per 100 mL (cfu/100mL) for the first week, on the order of 10^3 cfu/100mL for the second and third week, and on the order of 10^4 cfu/100mL for the fourth week. These levels of contamination have been observed in surface water sources in Guatemala (Elmore et al., 2005). Challenge water total coliform and *E. coli* levels were measured initially with Colilert Quantitray 2000® but after the first week were measured with Coliscan Easygel® in triplicate as the coliform concentrations grew too high to be quantified with the Quantitrays (which read up to 2419.6 cfu/100mL). Effluent water was tested for total coliforms and *E. coli* with Colilert Quantray 2000® each time the

concentration of coliforms in the challenge water increased to check for bacterial breakthrough.

Highly contaminated challenge water (on the order of 10^5 cfu/100mL) was passed through the filters to force failure in order to calculate a logarithmic reduction value (LRV) of the concentration of coliforms. LRV is a measure commonly used to measure the bacteria removal efficacy of POU water treatment systems (Van Halem et al., 2007; Sobsey et al., 2008; Clark and Elmore, 2011). The effluent from the reactors was tested for total coliforms and *E. coli* with Colilert Quantray 2000® to quantify the LRV.

3.4 PORE FORMER ANALYSIS

Hubbel et al. (in press) documented variable flowrates for ceramic filters composed of engineered clay bodies and sawdust, and that study concluded that sawdust size distribution and the distribution of the sawdust within the filters may be the source of the flowrate variability. It is reasonable to expect that the flowrates presented in this study would be less variable because clay and sawdust mixture is manipulated less relative the wedging process used by Hubbel to fabricate her experimental CPFs, and there would be less potential for uneven sawdust distribution during the formation of the filters used in this study. Wedging is a hand-mixing process by which sawdust is incorporated into the working body. This study instead used mechanical mixing, in which it is easier to tell when the mixture is homogenous. The shape and size of the sawdust used in this study was characterized by analyzing three samples using the Leica digital stereoscope, the ImageJ image analysis software, and a dial caliper. ImageJ software was used to calculate the

aspect ratio, roundness, and circularity as well as the area of the sawdust pieces. The dial caliper was used to measure heights of sawdust pieces.

Paper. Influence of carbon content on household ceramic water filter flowrate and disinfection efficacy

J.Y. Hahn, E.I.[1] and A.C. Elmore, Ph.D., P.E.[2]

[1]Graduate Student of Geological Engineering; Missouri University of Science and Technology; 129 McNutt Hall, 1400 N Bishop Ave, Rolla, MO 65409; email: jyhgy9@mst.edu

[2]Professor of Geological Engineering; Missouri University of Science and Technology; 129 McNutt Hall, 1400 N Bishop Ave, Rolla, MO 65409

Abstract

Ceramic pot filters are a point of use water source improvement technology which filter water by gravity through a porous ceramic media. Some filters in use contain carbon remnants left from the fugitive pore former as a dark carbon core. Using disk-shaped experimental ceramic filters produced in the lab to have varying levels of carbon, the percent carbon present was measured and a visual analysis method was developed to determine a representative statistic for the filters. A semi-logarithmic relationship was found between the physical carbon analysis method and the visual carbon analysis method. The experimental filters were installed in reactors and contaminated water was run through them over the course of four weeks. Flowrate and logarithmic reduction values (LRV) were determined for each filter at the end of the four weeks. No significant benefit was identified for the presence or the absence of carbon, however, a marginal benefit of complete burnout of carbon is a more focused grouping of flowrate and LRV, which could contribute to a more efficient manufacturing process and a more consistent final product.

Keywords: ceramic pot filter, water filtration, point of use, incomplete burnout

Introduction

According to the World Health Organization and the United Nations Children's Fund (WHO and UNICEF, 2014), 748 million people did not have access to improved drinking water sources in 2012. Improved drinking water sources can be a centralized system for a community or a point of use (POU) system designed to provide water for one household. POU treatment systems are an effective option in rural communities without a central improved water source because POU technologies require less infrastructure and initial expenditure, making the improved water available to the household sooner (Sobsey et al., 2008). One effective POU technology is the ceramic pot filter (CPF) (Hunter, 2009). CPFs are porous ceramic filters with a tapered cylindrical pot shape applied with colloidal silver or silver salt as a disinfectant. Water, poured into the pot-shaped filter, flows by gravity through the CPF and into a plastic bucket to be dispensed via a spigot for drinking. Van Halem et al. (2007) identifies the main bacterial removal mechanisms for CPFs as exclusion by pore size, exclusion by effective pore size (tortuosity), and deactivation of bacteria by contact with colloidal silver. These mechanisms can interact synergistically, which acts as a fourth removal mechanism.

The authors observed the CPF manufacturing process at a factory near Antigua, Guatemala. The raw materials used are clay, sawdust, and water. The sawdust, which is passed through a wire mesh to eliminate particles larger than a No. 8 sieve, acts as a fugitive pore former to increase porosity and permeability. Clay from Rabinal, Guatemala is mixed with the sieved sawdust at an approximate weight ratio of 6:1 clay-to-sawdust and wetted to create a working body. When it appears homogenous, the working body passes through an extruder to finalize mixing. The working body is then formed into a pot shape with a

mechanical press. The shaped CPFs are then set to dry completely on shelving in the open-air factory for 1 to 3 weeks before being fired in a propane-fired kiln in batches of approximately 200. The filters soaked in water overnight to saturate prior to a quality control flowrate test. The one-hour falling head test is conducted in duplicate to ensure that the flowrates of the filters are between 1 and 2 liters per hour. Filters that pass the test are painted inside and out with colloidal silver in solution.

The firing schedule used by the factory near Antigua, Guatemala leads to the presence of a black core of incompletely combusted sawdust (carbon) remaining in the filters. The firing process has a total duration of 7 to 8 hours. The kiln burner is operated for three hours to raise the temperature to 450 to 500^{o}C then turned off for 1.5 hours with the vents closed, which limits the oxygen in the kiln and induces a reducing atmosphere. The burner is turned on again, increasing the temperature to a maximum of 750^{o}C before the kiln is turned off and the top vents are opened for cooling. The open vents allow some burnout of carbon beginning from the outside of the CPFs; however, oxygen is limited and the burnout occurs slowly. Once the kiln temperature cools below the combustion point of the sawdust the burnout stops, leaving a carbon remnant core in the CPFs.

The factory describes the carbon remnants as activated carbon that should add to the removal of bacteria and improving the taste of the water. However, the Ceramics Manufacturing Working Group (2011) notes that additional research is needed to explore the influence of the carbon core on the efficacy and lifetime of the CPFs and recommends complete burnout for the most effective filters. This study investigates the carbon remnants in the CPFs, focusing on the influence of varying levels of carbon remnants in the filters

on short-term filter efficacy and flowrate as well as building a tool to visually evaluate the relative carbon content in a CPF.

Methods

The filters used in this study were manufactured on the Missouri University of Science and Technology campus from a synthetic clay body with a process that attempted to simulate the production process in the factory near Antigua, Guatemala. The clay body used was developed in an earlier study to resemble the clay from Rabinal, Guatemala used in the CPF factory (Hubbel et al., in press). Lower levels of iron in the clay developed by Hubbel et al. (in press) gave it a lighter color relative to the native clay from Rabinal which was determined preferable as the lighter color would make the dark carbon core more apparent for visual analysis. The sawdust was sieved through a No. 8 sieve and combined in a 6:1 weight ratio with the clay, then mixed with deionized water until homogenous. The filter shape chosen for this study is a disk shape, similar to that used by Oyandel-Craver and Smith (2007) and Ren and Smith (2013). Thirty disks were formed with a circular manual press set to the thickness of the bottom of the filters produced in Guatemala. The resulting disk-shaped filters had a diameter of 10 cm and a thickness of 2 cm. After pressing and before firing, the filters were allowed to dry for at least a week and spent at least 8 hours drying in a soils oven set at 100^{o}C. The filters in this study were not applied with colloidal silver in an effort to simplify the focus of the study because CPFs have been found effective even without silver present (Oyandel-Craver and Smith, 2007; Clark and Elmore 2011).

The filters were fired in an electric kiln in three separate firings with different atmospheres. The firing schedule (temperatures and times) was the same for each of the

firings, but the atmosphere was different for each firing. The firing schedule slowly increased the kiln temperature to 993^{o}C over the course of 14 hours before allowing it to cool back to room temperature. Ten filters were fired in each firing. For the mid-range atmosphere firing, oxygen was limited locally by placing the filters in a cordierite sagger box with a partial seal, and placing other combustible material (additional sawdust) in the box to partially scavenge oxygen that entered the box. The resulting atmosphere limited oxygen to result in incomplete burn out and leave some carbon remnants. For the reducing atmosphere firing, the process was repeated with additional combustible material in the sagger box and a thicker seal. The filters in this firing experienced less burnout than the first firing with more carbon remnants left in place. The oxidizing atmosphere firing was performed in air (without a sagger box), causing all of the sawdust to fully combust.

After firing, the filters that had incomplete combustion had more carbon remnants in the central region than around the edges because the oxygen was able to penetrate into the edges more than into the center. To obtain a more homogenous disk for testing, a smaller disk 5 cm in diameter was cut from the center of each disk.

The content of carbon was analyzed both visually and physically. The physical investigation was performed by powdering approximately 5 grams of the inner perimeter of the 10 cm disks from which the 5 cm disks were removed. The powder was then sent to the University of Missouri Extension Soil Testing Laboratory in Columbia, Missouri for total carbon analysis by combustion using an Elementar Vario MAX Carbon/Nitrogen Analyzer. Visual testing was performed by taking 3 images along the circumference of the filter disks with both a Leica S8APO digital stereoscope and a HiROX KH-8700 digital microscope. The two instruments were used in order to have two different image sets of

the same physical filters so that they could be compared to validate the developed visual methodology. The images taken with each digital imaging device used the same shutter speed, light settings, and image parameters. Each image was cropped to include only the filter material and then converted to greyscale. Matlab code was written to import the images as an array with a value (0 for black to 255 for white) for each pixel of the image, then to return the median value of the array to get a representative tone value for the image. The values were averaged for the three images of each filter to obtain a representative tone for that filter.

Shards from production filters made at the factory in Guatemala were also visually analyzed for carbon content to show that they contain carbon and that they contain variable amounts of carbon. These CPFs were observed to have a carbon core in the interior and full burnout at the surface. Three images were taken from the surface of the CPF shard to be representative of a filter that had experienced full burnout. Seven images were taken of a cross-section of the filters to show the carbon core. These images were taken on both the Leica stereoscope and the HiROX microscope, and were processed in the same way as the experimental filter images to produce a representative value for each image. A paper standard was used to identify differences between the Leica stereoscope and the HiROX microscope images. The standard had six printed blocks of color: white, white darker 5 percent, white darker 15 percent, white darker 50 percent, black lighter 25 percent, and black. An image was taken of each color block on each imaging device. These images were processed in the same way as the production filter images and the experimental filter images to identify a representative tone value for each image.

The porosity of the filters was determined in order to find the pore volume for the filters. A modified Archimedes method (ASTM C830-00) was used to characterize the apparent porosity of two experimental filters, one with complete burnout and one with incomplete burnout (with apparent high carbon content). Instead of using a vacuum and pressure chamber to saturate the samples, each sample was left to soak submerged in water for at least 18 hours to achieve saturation. This procedure is similar to the procedure followed by the CPF factory in Guatemala to saturate their filters before flowrate testing.

Six filters from each firing were affixed inside plastic tubes, for a total of 18 experimental reactors. The filters were disinfected according to the procedure used by Clark and Elmore (2011) with three pore volumes (45 mL total) of bleach water solution (0.08 mL/L chlorine). Once the filters were disinfected, each filter was filled with a sodium thiosulfate solution (0.25 mg/L) to remove any residual chlorine. The effluent water was tested for total chlorine with a Hach Total Chlorine field kit (CN-66T) to ensure that all chlorine was removed. If the test came back with any presence value for total chlorine, additional sodium thiosulfate solution was passed through the filter to eliminate the chlorine until the Total Chlorine low range test was below the detection limit. A presence/absence Colilert® coliform test analyzed the effluent from each filter to ensure that there were no coliforms present in the effluent from the filters before testing began.

To test the filters, a simulated contaminated surfaced water was produced using influent from the wastewater treatment plant (WWTP) in Rolla, Missouri. The WWTP influent was mixed with tap water to create the testing influent water ("challenge" water) for the filters, which was passed through the filters for four weeks. The challenge water was on the order of 10^2 colony forming units per 100 mL (cfu/100mL) for the first week,

on the order of 10^3 cfu/100mL for the second and third week, and on the order of 10^4 cfu/100mL for the fourth week. These levels of contamination have been observed in surface water sources in Guatemala (Elmore et al., 2005). Challenge water total coliform and *E. coli* levels were measured initially with Colilert Quantitray 2000® but after the first week were measured with Coliscan Easygel® in triplicate as the coliform concentrations grew too high to be quantified with the Quantitrays (which read up to 2419.6 cfu/100mL). Effluent water was tested for total coliforms and *E. coli* with Colilert Quantray 2000® each time the concentration of coliforms in the challenge water increased to check for bacterial breakthrough.

Highly contaminated challenge water (on the order of 10^5 cfu/100mL) was passed through the filters to force failure in order to calculate a logarithmic reduction value (LRV) of the concentration of coliforms. LRV is a measure commonly used to measure the bacteria removal efficacy of POU water treatment systems (Van Halem et al., 2007; Sobsey et al., 2008; Clark and Elmore, 2011). The effluent from the reactors was tested for total coliforms and *E. coli* with Colilert Quantray 2000® to quantify the LRV.

Results and Discussion

The Leica and HiROX median greyscale standard readings were plotted on a scattergram, and the slope of the best fit linear trend line was 0.872 with an R^2 value of 0.95. This indicates that both instruments gave relatively similar readings. The scattergram results for the production filters were 1.41 slope and $R^2 = 0.92$, which indicated that the instruments gave similar readings for imaging a heterogeneous, porous surface.

The experimental filter images were taken at varied points along the circumference of the image in order to gain a representative tone for the filter in its entirety. The

scattergram analysis for the experimental filters resulted in a slope of 1.13 and an R^2 value of 0.77 which reflect the variability of the carbon in the filters. Summary statistics for both Leica and HiROX images appear in Table 1. The variability of the carbon remnants in the experimental filters simulates the uneven distribution of carbon remnants observed in the production filters.

Table 1: Summary Statistics for Study Analytes

		Carbon	Visual Median Tone		Flowrate (mL)		
Group	Statistic	Content (%)	HiROX	Leica	Initial	Final	LRV
Oxidizing	Mean	0.0284	172	190	44	29	3.66
	Standard Deviation	0.0064	17.7	3.2	5.8	4.9	0.48
	Coefficient of Variation	0.224	0.103	0.017	0.131	0.167	0.131
Mid-Range	Mean	0.216	110	92	49	29	4.09
	Standard Deviation	0.252	40.8	49.0	5.9	7.7	0.41
	Coefficient of Variation	1.166	0.370	0.533	0.121	0.260	0.101
Reducing	Mean	1.423	57	39	63	35	2.84
	Standard Deviation	0.274	10.9	11.4	5.2	8.1	0.83
	Coefficient of Variation	0.193	0.190	0.290	0.083	0.234	0.294
Overall	Mean	0.556	113	107	52	31	3.52
	Standard Deviation	0.667	54.1	69.9	9.6	7.1	0.79
	Coefficient of Variation	1.200	0.479	0.652	0.185	0.228	0.225

The total carbon content was determined for each of the experimental filters, and summary statistics appear in Table 1. The oxidizing firing group had the lowest carbon content of the three groups. The mid-range firing group was a highly varied group with a coefficient of variation (CV) of 1.17, the only group with a CV greater than 1. Three of the filters in the mid-range group had very low carbon levels similar to those found in the oxidizing group, which is attributed to the position of these filters closer to an oxygen source in the kiln during firing. These three filters were located at the top of the box with greater exposure to oxygen and thus greater burnout of the fugitive pore former. The other

three filters in this group were located nearer to the bottom of the box where less oxygen was present, thus preventing the sawdust from fully combusting. The reducing group exhibited the highest carbon content and the lowest CV.

A comparison of the visual carbon analysis results (median tone values) and the physical carbon analysis results (percent total carbon) appears in Figure 1. There is an apparent logarithmic relationship between the total carbon content and the median tone value. The coefficient of determination between the carbon content and the median tones from the HiROX image set was 0.75; the coefficient of determination for the carbon content

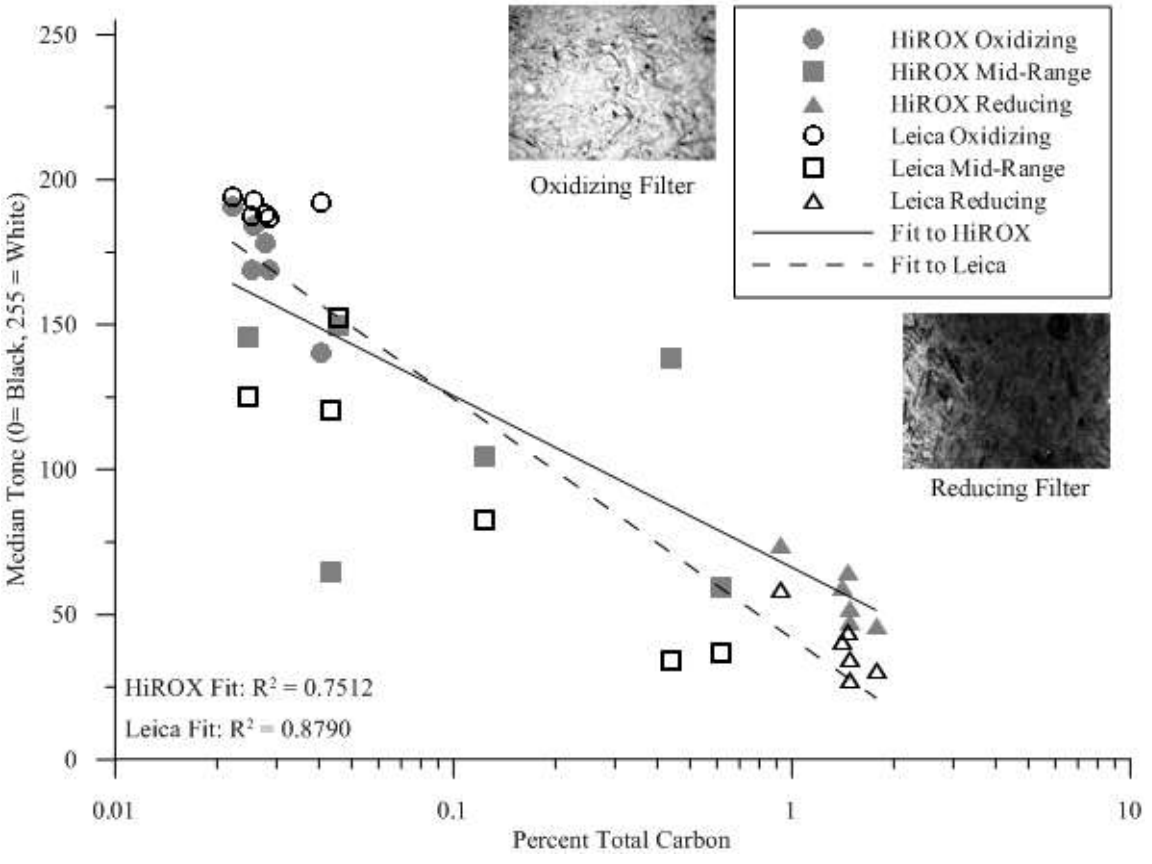

Figure 1: Physical carbon analysis vs visual carbon analysis.

and the median tones from the Leica image set was 0.88. Both of these values indicate that a relationship is present, but because of the better correlation with the Leica images that data was used as the representative visual carbon data.

The porosity was measured for one oxidizing filter and one reducing filter in order to gain a general understanding of the difference in porosity. The reducing filter chosen was one with a very dark appearance indicating a high level of carbon so that the influence of the carbon on the porosity could be evaluated. The apparent porosities measured in the oxidizing and reducing filters were 44.3 percent and 43.8 percent, respectively, indicating that porosity was similar for the filter groups.

The flowrates for each filter were measured twice, once at the beginning and once at the end of the experimentation. All 18 filters experienced a drop in flowrate over the study period. As shown in Table 1, the CV was greater for each group at the final measurement than at the initial measurement, indicating that the use of the filters lead to a more variable flowrate. Flowrate means were similar for the oxidizing and mid-range groups but higher for the reducing group at both the initial and final measurements. Initially, the oxidizing group flowrates showed the greatest variation (CV of 0.131) and the reducing group flowrates showed the least variation (CV of 0.083), but after four weeks of use the oxidizing group had significantly less variation (CV of 0.167) compared to the mid-range (CV of 0.260) and reducing groups (CV of 0.234).

The LRV were calculated by taking the difference between the $\log_{10}$ of the influent coliform concentration (cfu/100mL) and the $\log_{10}$ of the effluent coliform concentration (cfu/100mL). As shown in Figure 2, the semi-logarithmic relationship between the percent

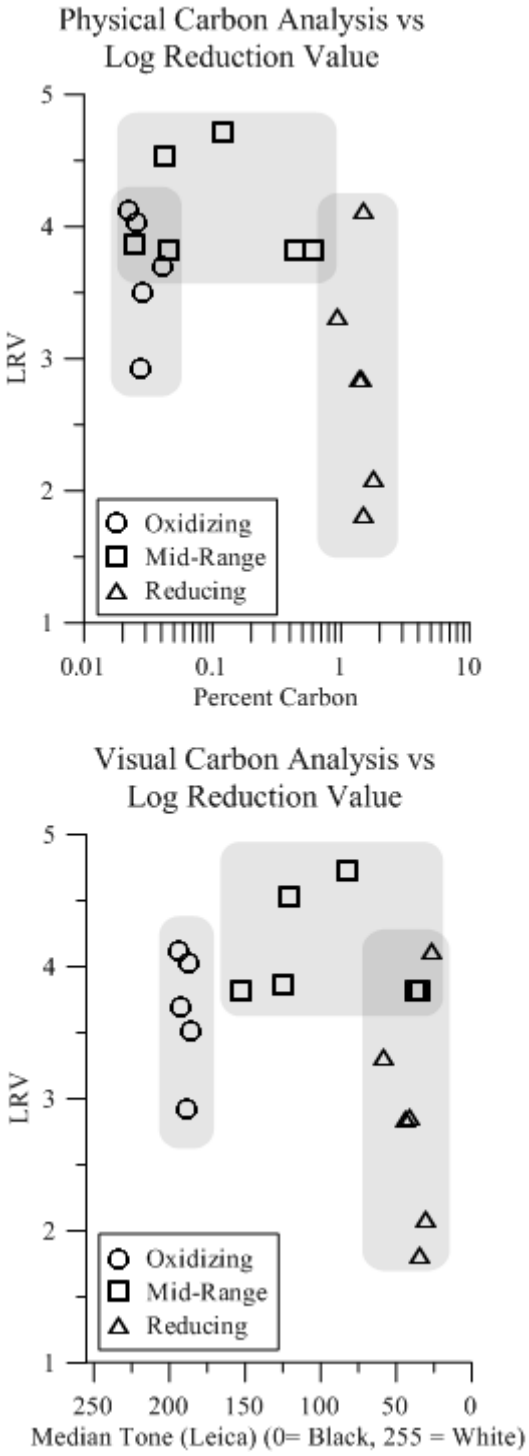

Figure 2: Carbon analysis vs LRV.

carbon and the median image tone leads to very similar graphs of percent total carbon versus LRV and Leica median tone value versus LRV. The LRV ranges overlapped for the reducing and oxidizing group with the reducing group having a larger LRV range. The LRV CV was also larger for the reducing group (0.29) relative to the oxidizing group CV (0.13). The regions highlighted on the graph show that the oxidizing, mid-range, and reducing groups occupy distinct regions on the graph.

Flowrate is a commonly used quality control measure in many CPF factories (Ceramics Manufacturing Working Group, 2011), meaning that a relationship between flowrate and efficacy would be expected (namely, that filters with higher flowrates could pass more coliforms), however, a scattergram analysis of the data from this experiment did not indicate any relationship between final flowrate and LRV. Figure 3 shows that the flowrate was also relatively insensitive to the carbon content. The regions highlighted in

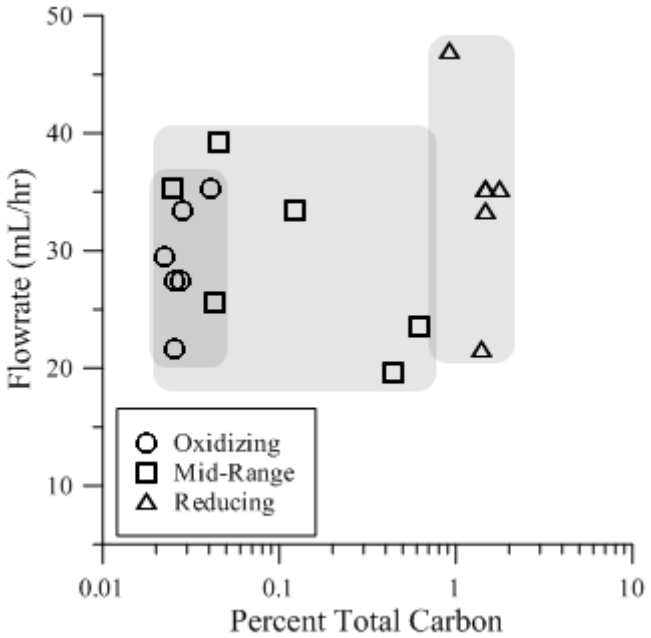

Figure 3: Physical carbon analysis vs flowrate.

Figure 3 have similar size and placement to those that appear in Figure 2, indicating that the firing groups again had distinct behaviors. The range of flowrates for the oxidizing group overlapped with the range for the reducing group but were more focused, again indicating a potential for better control of CPF parameters when complete burnout is achieved.

Conclusion

The visual carbon analysis method developed in this study has potential as an efficient and economical method of evaluating the content of carbon present in CPFs. Raw median tones could be used to identify relative qualitative carbon content or standards could be tested for carbon content and the process could be used to quantify carbon content more rapidly than transmitting samples to offsite analytical laboratories.

No direct significant benefit was observed for either the presence or the absence of carbon remnants in terms of flowrate or disinfection efficacy. A marginal benefit of complete burnout of pore former was that smaller variations were observed in the flowrate and LRV of those filters, which could mean that these parameters could be controlled more readily. This could lead to fewer filters being rejected during quality control flowrate testing, making the production process more efficient, as well as greater reliability of the CPFs' efficacy. Another potential benefit of the absence of carbon remnants is to reduce the potential for biofouling of the filter, as the carbon could theoretically support growth of bacteria (LeChavallier et al., 1984; Camper et al., 1985).

This study examined short-term effects of the residual carbon in CPFs. A long-term study on the effects of residual carbon on CPF performance that included effective CPF

lifetime along with flowrate and efficacy values may add to the understanding of the effects of the carbon remnants on filter performance.

Acknowledgements

The authors are grateful to the management and staff of the CPF factory near Antigua, Guatemala, who provided the opportunity for observation of their production process. The Missouri S&T Geological Engineering program provided financial support for this research. The authors are also grateful to Dr. Mary Reidmeyer of the Ceramic Engineering program at Missouri S&T for sharing her extensive knowledge and expertise.

References

Camper A.K., LeChevallier M.W., Broadaway S.C., and McFeters G.A. 1985 Growth and persistence of pathogens on granular activated carbon filters. *Applied and Environmental Microbiology*, 50(6), 1378-1382.

Ceramics Manufacturing Working Group 2011 *Best Practice Recommendations for Local Manufacturing of Ceramic Pot Filters for Household Water Treatment* 1st edn, Center for Disease Control and Prevention, Atlanta, GA, USA.

Clark K.N. and Elmore A.C. 2011 Bacteria removal effectiveness of ceramic pot filters not applied with colloidal silver. *Water Science and Technology: Water Supply*, 11(6), 765-772.

Elmore A.C., Miller G.R., Parker B. 2005 Water quality in Lemoa, Guatemala. *Environmental Geology*, 48, 901-907.

Hubbel L., Elmore A.C., Reidmeyer M. (in press) Comparison of a native clay soil and an engineered clay used in experimental ceramic pot filter fabrication. *Water Science and Technology: Water Supply*.

Hunter P.R. 2009 Household water treatment in developing countries: comparing different intervention types using meta-regression. *Environmental Science and Technology*, 43, 8991-8997.

LeChevallier M.W., Hassenauer T.S., Camper A.K. and McFetters G.A. 1984 Disinfection of bacteria attached to granular activated carbon. *Applied and Environmental Microbiology*, 48(5), 918-923.

Oyandel-Craver V.A. and Smith J.A. 2007 Sustainable colloidal-silver-impregnated ceramic filter for point-of-use water treatment. *Environmental Science and Technology*, 42, 927-933.

Ren D. and Smith J.A. 2013 Retention and transport of silver nanoparticles in a ceramic porous medium used for point-of-use water treatment. *Environmental Science and Technology*, 47, 3825-3832.

Sarikaya A. and Dogan F. 2012 Effect of various pore formers on the microstructural development of tape-cast porous ceramics. *Ceramics International*, 39, 403-413.

Sobsey M.D., Stauber C.E., Casanova L.M., Brown J.M., and Elliott M.A. 2008 Point of use household drinking water filtration: a practical, effective solution for providing sustained access to safe drinking water in the developing world. *Environmental Science and Technology*, 42, 4261-4267.

Standard Test Methods for Apparent Porosity, Liquid Absorption, Apparent Specific Gravity, and Bulk Density of Refractory Shapes by Vacuum Pressure 2011, C830-00, American Society for Testing and Materials, West Conshohocken, PA, USA.

van Halem D., Heijman S.GJ., Soppe A.I.A., van Dijk J.C. and Amy G.L. 2007 Ceramic silver-impregnated pot filters for household drinking water treatment in developing countries: material characterization and performance study. *Water Science and Technology: Water Supply*, 7(5-6), 9-17.

World Health Organization and United Nations Children's Fund 2012 *Progress on Sanitation and Drinking-water: 2012 Update*. Geneva, Switzerland.

SECTION

4. RESULTS AND DISCUSSION

Hubbel et al. (in press) noted highly variable flowrate and surmised that it was likely caused by inconsistencies in the sawdust as a pore former. The shape and size of the sawdust used in this study was characterized by analyzing three samples using the Leica digital stereoscope, the ImageJ image analysis software, and a dial caliper. The dial caliper was used to measure heights of sawdust pieces. ImageJ software was used to measure area, aspect ratio, and circularity. Aspect ratio is a ratio of the longest diameter to the shortest diameter with high values indicating a great difference in the axes, with a value of 1.0 for a shape that can be inscribed in a circle and increasing values for shapes that can be inscribed in a more elongated ellipse. Circularity is a measure of how closely a circle and ranges from 0.0 (elongated) to 1.0 (circular). The results of these analyses are included in Appendix G. The overall average particle size from the three photographs was 260.5 μm^2 with a standard deviation of 394.1 μm^2 giving a coefficient of variation (CV) of 1.51, which indicates a large variability in the cross sectional area of the particles. The mean aspect ratio was 2.38 and the mean circularity was 0.35; both of these values indicate that the average sawdust particle had an elongated shape.

Figure 4.1 shows an image of the sawdust. Appendix G includes all three images taken of the sawdust as well as a summary of the particle size distribution and shape characteristics. The sawdust particle dimensions are significantly larger than the CPF target pore size diameter of 1 μm identified by Lantagne (2001) or even the acceptable range of

Figure 4.1: Sawdust used as pore former.

6 to 31 μm for silver salt-enhanced ceramic candle filters (Basu, 1982). Van Halem et al. (2007) discusses the use of mercury intrusion porosimetry to characterize pore size distribution in CPFs, but that method includes the assumption of cylindrical pores and circular pore openings. Clearly, the information presented in Figure 5.1 indicates that it is highly unlikely that the subject sawdust would create such regular pores, but the sawdust analysis does not characterize the final pore size and shape distribution within the completed ceramic filters.

5. CONCLUSION

5.1 VISUAL CARBON ANALYSIS

The visual carbon analysis method developed in this study has potential as an efficient and economical method of evaluating the content of carbon present in CPFs. Raw median tones could be used to identify relative qualitative carbon content or standards could be tested for carbon content and the process could be used to quantify carbon content more rapidly than transmitting samples to offsite analytical laboratories.

5.2 EFFECTS OF CARBON ON PERFORMANCE PARAMETERS

No direct significant benefit was observed for either the presence or the absence of carbon remnants in terms of flowrate or disinfection efficacy. A marginal benefit of complete burnout of pore former was that smaller variations were observed in the flowrate and LRV of those filters, which could mean that these parameters could be controlled more readily. This could lead to fewer filters being rejected during quality control flowrate testing, making the production process more efficient. It could also lead to a more consistent product for consumers.

5.3 PORE FORMER ANALYSIS

The observations made about the sawdust in this study support the conclusion of Hubbel et al. (in press) that the sawdust as a pore former may be a source of variability in flowrate. The sawdust analysis also indicates that the characterization of porosity

parameters may be a data gap as the assumptions of porosimetry methods used in previous studies may not be satisfied by the pores formed from irregular sawdust material.

5.4 RECOMMENDATIONS FOR FUTURE WORK

This study examined short-term effects of the residual carbon in CPFs. A long-term study on the effects of residual carbon on CPF performance that included effective CPF lifetime along with flowrate and efficacy values may add to the understanding of the effects of the carbon remnants on filter performance.

The highest carbon contents found in this study were less than two percent. These levels are low and may not be representative of production filters. An investigation of the levels of carbon in production flowrates may be useful to future investigation of the effects of carbon remnants.

APPENDIX A

PHYSICAL AND VISUAL CARBON ANALYSIS DATA

Visual Analysis of Experimental Filters using the Leica Stereoscope and the HiROX Microscope

Leica Stereoscope Median Tone Values				
	Visual Median Tone			
Disk ID	1	2	3	Average
O1	183.08	201.53	191.46	192.03
O2	197.20	188.89	192.18	192.76
O3	191.73	195.50	195.25	194.16
O4	192.61	190.63	180.98	188.07
O6	185.60	184.36	189.61	186.52
O7	183.89	189.59	189.25	187.57
M1	70.74	83.26	94.44	82.82
M2	135.37	133.28	106.26	124.97
M3	129.31	135.94	95.91	120.39
M4	41.44	41.28	27.99	36.90
M5	147.61	133.62	175.92	152.38
M6	21.80	36.00	45.07	34.29
R10	30.11	26.76	24.53	27.13
R9	49.26	63.43	19.06	43.92
R8	43.29	40.43	21.24	34.99
R7	72.90	29.16	19.67	40.58
R6	57.62	75.75	43.46	58.94
R5	49.39	24.27	17.82	30.49

HiROX Microscope Median Tone Values				
	Visual Median Tone			
Disk ID	1	2	3	Average
O1	135.13	145.06	140.09	140.09
O2	175.00	187.05	190.31	184.12
O3	184.84	190.23	196.82	190.63
O4	183.73	179.97	169.87	177.86
O6	166.72	175.85	164.19	168.92
O7	185.28	160.82	159.92	168.67
M1	93.28	107.38	112.64	104.43
M2	150.36	149.55	137.35	145.75
M3	92.25	47.52	54.30	64.69
M4	54.01	70.98	51.93	58.97
M5	140.02	162.28	146.30	149.53
M6	121.03	142.81	150.16	138.00
R10	51.62	61.70	43.59	52.31
R9	80.27	76.37	38.15	64.93
R8	47.77	52.32	41.91	47.33
R7	37.19	52.84	88.43	59.49
R6	65.53	92.43	63.27	73.74
R5	36.19	68.79	32.47	45.82

Visual Analysis of Production Filters using the Leica Stereoscope and the HiROX Microscope

Production Filter Designation	HiROX Median Tone	Leica Median Tone
B1	83.31	102.36
B2	89.43	120.53
B3	96.28	114.01
1	49.00	57.98
2	54.43	63.23
3	56.28	61.65
4	51.94	56.13
5	71.50	90.56
6	52.24	53.88
7	73.01	71.52

* B indicates a "baseline" image taken at a location with full burnout

Visual Analysis of Standards using the Leica Stereoscope and the HiROX Microscope

Standard Designation	HiROX Median Tone	Leica Median Tone
S1	24.07	35.78
S2	215.27	223.76
S3	117.15	163.71
S4	41.59	56.98
S5	221.81	223.82
S6	248.65	223.83

Total Carbon Content of Experimental Filters

Disk ID	Percent Carbon
O1	0.041
O2	0.026
O3	0.022
O4	0.028
O6	0.029
O7	0.025
M1	0.123
M2	0.025
M3	0.043
M4	0.619
M5	0.046
M6	0.441
R10	1.481
R9	1.462
R8	1.481
R7	1.412
R6	0.928
R5	1.773

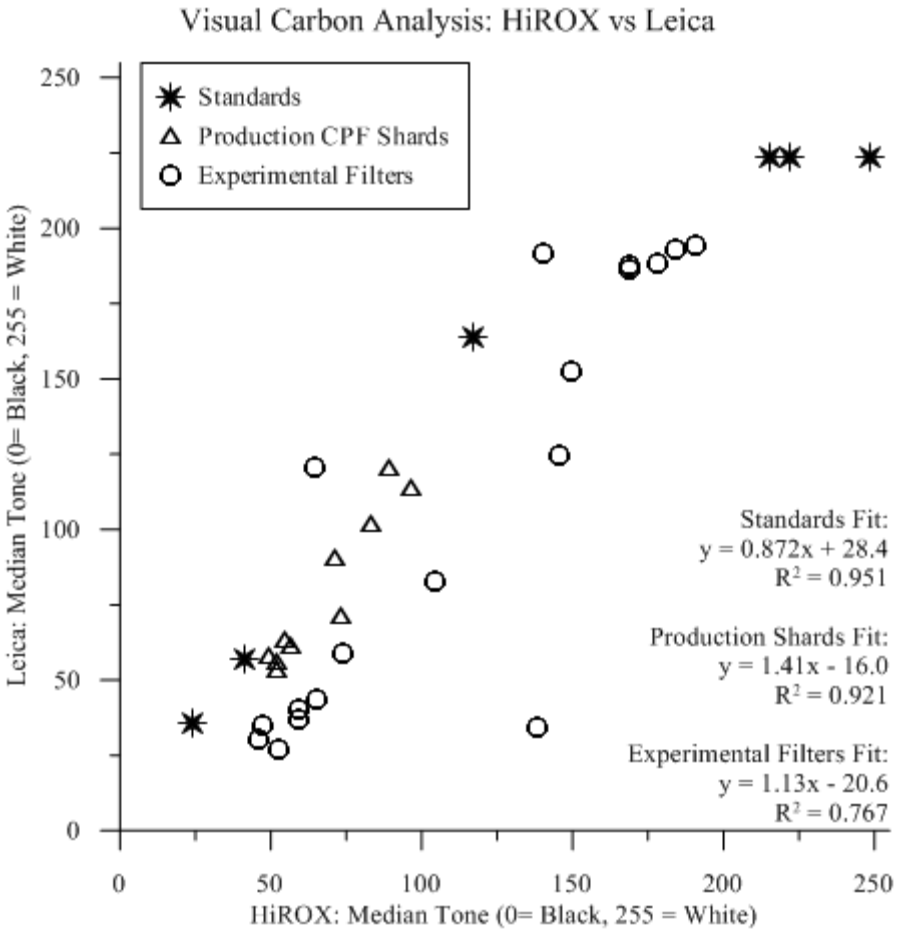
Visual Carbon Analysis: HiROX vs Leica
Standards
Production CPF Shards
Experimental Filters
Standards Fit:
y = 0.872x + 28.4
R² = 0.951
Production Shards Fit:
y = 1.41x - 16.0
R² = 0.921
Experimental Filters Fit:
y = 1.13x - 20.6
R² = 0.767
Leica: Median Tone (0= Black, 255 = White)
HiROX: Median Tone (0= Black, 255 = White)
0
50
100
150
200
250

APPENDIX B

INFLUENT COLIFORM CONCENTRATIONS

Influent Coliform Concentrations for Experimental Filters

		Influent Bacteria (CFU/100mL)	
Date	Time	Total Coliforms	*E. coli*
28-Jan	1600	(chlorination)	
29-Jan	1500	(dechlorination)	
31-Jan	1730	2	< 1
2-Feb	1200	1	< 1
3-Feb	1600	>2419.6	218
5-Feb	1400	< 1	< 1
7-Feb	1000	3.1	3.1
8-Feb	2100	920.8	290.9
9-Feb	2200	>2419.6	1119.9
11-Feb	1530	2419.6	260.3
12-Feb	2000	12315.8	916.6
14-Feb	1200	3270.5	959.0
15-Feb	1215	2567.5	726.8
16-Feb	1700	16091.1	1310.4
17-Feb	1200	11915.5	1497.8
19-Feb	1100	10189.8	1398.6
22-Feb	1100	452324.9	27086.1
25-Feb*	1300	13207.7	58.5
28-Feb	1630	104186.0	110.4

*25 February was the date when the 22 February water was tested. The influent water was resampled to account for the natural death of bacteria over time.

APPENDIX C

FLOWRATES OF EXPERIMENTAL FILTERS

Flowrates of Experimental Filters

Disk ID	Flowrate 5 Feb (mL/hr)	Flowrate 22 Feb (mL/hr)
O1	39.27	77.11
O2	43.20	84.82
O3	43.20	84.82
O4	51.05	100.24
O6	51.05	100.24
O7	37.31	73.25
M1	49.09	96.38
M2	49.09	96.38
M3	56.94	111.80
M4	41.23	80.96
M5	53.01	104.09
M6	43.20	84.82
R10	58.90	115.66
R9	60.87	119.51
R8	60.87	119.51
R7	58.90	115.66
R6	72.65	142.65
R5	62.83	123.37

APPENDIX D

EFFLUENT COLIFORM CONCENTRATIONS

Effluent Coliform Concentrations from Experimental Filters and Initial Disinfection Confirmation

Initial Testing		Effluent Date	4-Feb		6-Feb		9-Feb		11-Feb		12-Feb		22-Feb		25-Feb *		28-Feb*	
28-Jan	29-Jan	Influent Date	3-Feb		5-Feb		8-Feb		9-Feb		11-Feb		20-Feb		22-Feb		27-Feb	
Cl (mg/L)	Coliform (P/A)	Disk ID	TC	*E. coli*	TC	*E. coli*	TC	*E. coli*	TC	*E. coli*	TC	*E. coli*	TC	*E. coli*	TC	*E. coli*	TC	*E. coli*
<0.04	A	O1	1	0	0	0	0	0	0	0	0	0	0	0	0	0	21.1	0
<0.04	A	O2	0	0	-	-	0	0	0	0	0	0	0	0	0	0	0	0
<0.04	A	O3	0	0	-	-	0	0	0	0	0	0	0	0	1	0	34.1	0
<0.04	A	O4	0	0	-	-	0	0	0	0	0	0	0	0	0	0	123.6	7.3
<0.04	A	O6	0	0	-	-	0	0	0	0	0	0	0	0	4.1	1	>2419.6	344.8
<0.04	A	O7	0	0	-	-	0	0	0	0	0	0	0	0	0	0	9.7	0
<0.04	A	M1	2	2	0	0	0	0	0	0	0	0	1	1	0	0	2	0
<0.04	A	M2	0	0	-	-	0	0	0	0	0	0	0	0	0	0	14.4	2
<0.04	A	M3	0	0	-	-	0	0	0	0	0	0	0	0	0	0	3.1	1
<0.04	A	M4	0	0	-	-	0	0	0	0	0	0	3.1	1	2	0	0	0
<0.04	A	M5	0	0	-	-	0	0	0	0	0	0	0	0	2	1	>2419.6	0
<0.04	A	M6	0	0	-	-	0	0	0	0	0	0	0	0	2	0	0	0
<0.04	A	R10	0	0	-	-	0	0	0	0	0	0	0	0	1	0	2	1
<0.04	A	R9	0	0	-	-	0	0	0	0	0	0	1	0	18.9	5.2	7.5	5.2
<0.04	A	R8	0	0	-	-	0	0	0	0	0	0	6.3	4.1	201.4	53.8	24.1	2
<0.04	A	R7	0	0	-	-	0	0	0	0	0	0	0	0	18.5	7.4	4.1	0
<0.04	A	R6	0	0	-	-	0	0	0	0	0	0	3.1	3.1	6.3	3.1	90.9	6.3
<0.04	A	R5	0	0	-	-	0	0	0	0	0	0	9.7	9.6	106.7	65.7	4.1	0

All coliform quantities are in CFU/100mL.

APPENDIX E

LOGARITHMIC REDUCTION VALUES

Experimental Filters: Logarithmic Reduction Values

Disk ID	LRV
O1	3.69
O2	*
O3	4.12
O4	2.93
O6	3.51
O7	4.03
M1	4.72
M2	3.86
M3	4.53
M4	3.82
M5	3.82
M6	3.82
R10	4.12
R9	2.84
R8	1.82
R7	2.85
R6	3.32
R5	2.09

* Filter O2 did not experience breakthrough, and thus a LRV value could not be calculated.

APPENDIX F

MATLAB CODE

The code below was used to find the median tone of grayscale images.

```
%%%%%%%%%%%%%%%%%%%%%%%%%%%%%%%%%%%%%%%%%%%%%%%%%%%%%%%%%%%%%%%%%%%%%%%
%%%                Photo Analysis                                    %%%
%%%                                                                  %%%
%%% Code prints histogram of tone values and                         %%%
%%%       outputs color data                                         %%%
%%%                                                                  %%%
%%%                                                Jessie Hahn       %%%
%%%%%%%%%%%%%%%%%%%%%%%%%%%%%%%%%%%%%%%%%%%%%%%%%%%%%%%%%%%%%%%%%%%%%%%

clear;
clc;

%% Import image from file using filename
Img = imread('[filename].tif');

[m,n,o] = size(Img);

%% Convert image to 2-D array (discard any extra data)
for i = 1:m;
    for j = 1:n;
        Img2D(i,j) = Img(i,j,1);
    end
end

%% Generate a historgram of grayscale intensities (tones)(0-255)
imhist(Img2D);
[counts,color] = imhist(Img2D);
stem(color,counts);

%% Find the median tone
x=[color,counts];

y = gmedian(x)
```

APPENDIX G

PORE FORMER ANALYSIS

Image 1 Sawdust Characteristics			
Particle Count	Area (μm^2)	Aspect Ratio	Circularity
1	6.255	3.859	0.018
2	9.186	1.905	0.01
3	8.442	1.506	0.009
4	8.661	1.517	0.009
5	14.697	1.608	0.008
6	9.536	1.676	0.01
7	5.468	3.718	0.016
8	7.217	1.903	0.013
9	18.765	1.652	0.005
10	5.205	1.654	0.005
11	8.880	1.301	0.011
12	15.222	2.07	0.006
13	8.180	2.606	0.012
14	5.861	3.596	0.014
15	7.174	1.569	0.004
16	5.293	4.135	0.004
Mean	9.0	2.27	0.010
Std Deviation	3.9	0.98	0.004

Sawdust Image 1

Image 2 Sawdust Characteristics			
Particle Count	Area (μm^2)	Aspect Ratio	Circularity
1	420.271	1.815	0.235
2	101.000	2.85	0.113
3	15.703	3.479	0.133
4	65.525	5.034	0.137
5	174.136	1.625	0.268
6	6.386	1.636	0.609
7	443.848	1.684	0.197
8	844.960	1.325	0.354
9	1141.267	1.251	0.172
10	1340.161	2.268	0.155
11	5.162	1.253	0.369
12	9.667	4.165	0.23
13	80.004	5.282	0.223
14	1320.302	1.806	0.184
15	186.121	1.386	0.2
16	478.448	1.133	0.297
17	95.838	4.821	0.192
Mean	395.8	2.52	0.239
Std Deviation	473.7	1.46	0.120

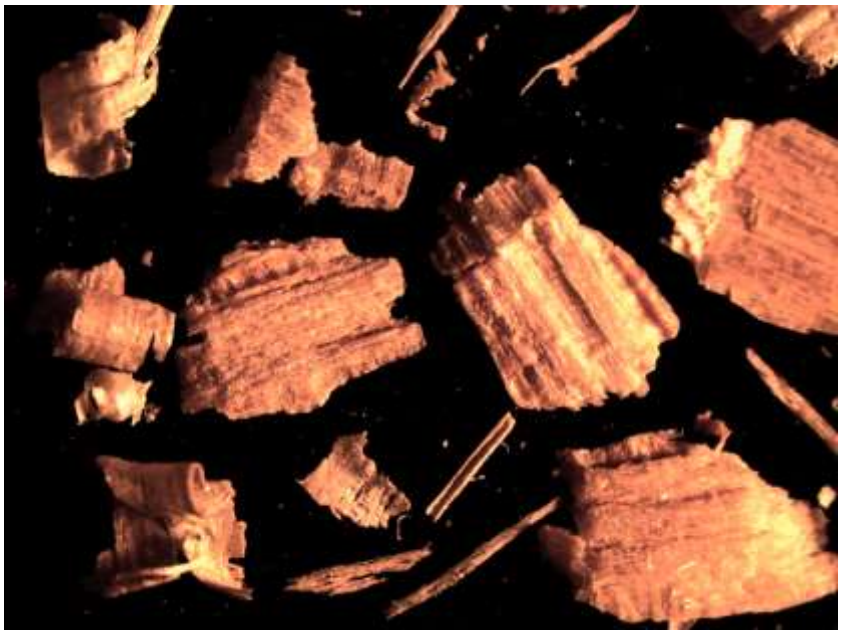

Sawdust Image 2

Image 3 Sawdust Characteristics			
Particle Count	Area (μm^2)	Aspect Ratio	Circularity
1	353.915	2.221	0.19
2	58.483	2.179	0.286
3	1270.480	2.999	0.228
4	7.830	1.733	0.591
5	579.141	2.222	0.145
6	746.891	1.499	0.204
7	779.303	1.639	0.188
8	865.825	1.464	0.276
9	501.106	1.971	0.581
10	122.040	1.354	0.174
11	6.911	1.615	0.757
12	172.343	6.518	0.285
13	73.836	2.048	0.327
14	88.271	4.263	0.183
15	4.549	1.63	0.814
Mean	375.4	2.36	0.349
Std Deviation	395.4	1.37	0.223
Overall Statistics (all particles in 3 images)			
Mean	260.5	2.38	0.197
Std Deviation	394.1	1.27	0.199

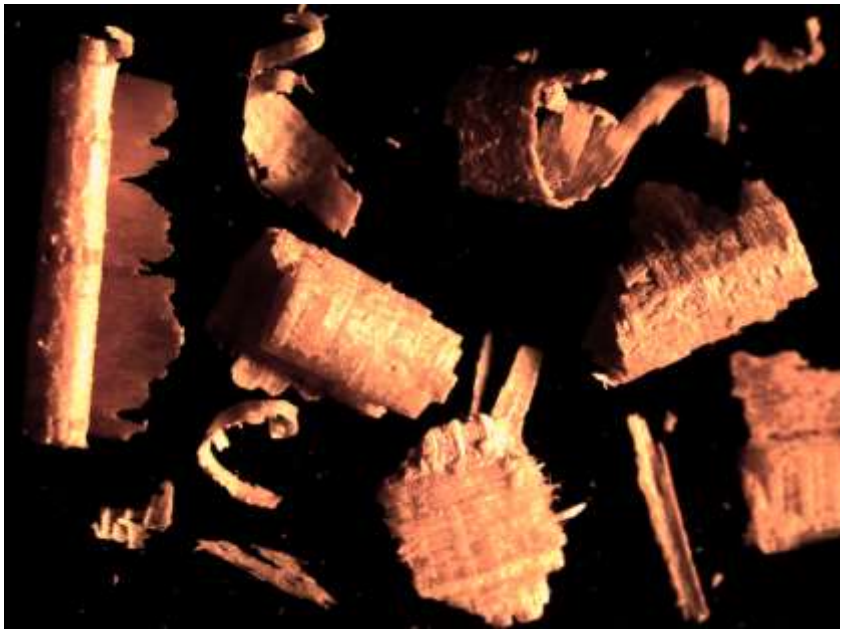

Sawdust Image 3

Sawdust Heights Measured with a Dial Caliper

Count	Height (mm)
1	1.32
2	1.91
3	1.65
4	0.51
5	1.91
6	2.01
7	1.07
8	1.55
9	1.52
10	0.38
11	1.57
12	2.44
13	0.64
14	1.83
15	1.42
16	1.45
17	0.84
18	0.66
19	0.41
20	2.11
21	1.88
22	1.27
23	2.13
24	1.98
25	1.35

APPENDIX H

FILTER IMAGES USED FOR ANALYSIS ON CD-ROM

A few sample images of experimental filters, production filters, and standards appear below. All images analyzed in this study are included with this thesis on a CD-ROM.

OXIDIZING GROUP EXPERIMENTAL FILTERS

HiROX image of filter O4

Leica image of filter O4

REDUCING GROUP EXPERIMENTAL FILTERS

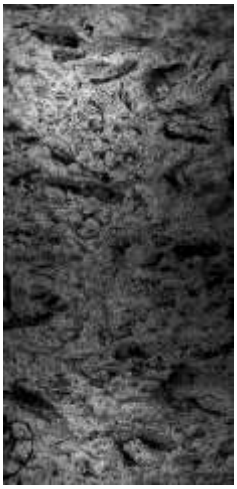

HiROX image of filter R9

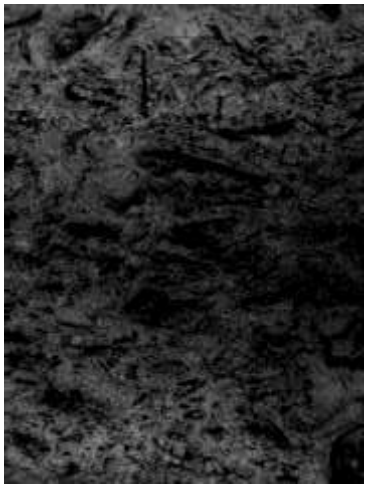

Leica image of filter R9

PRODUCTION FILTERS

HiROX image of Location 6

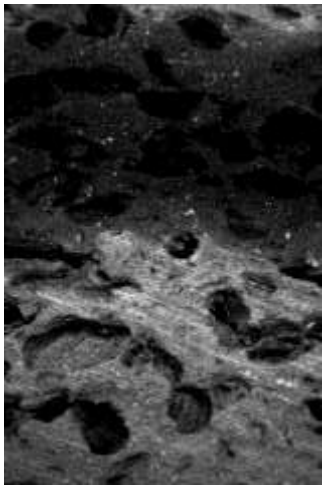

Leica image of Location 6

STANDARDS

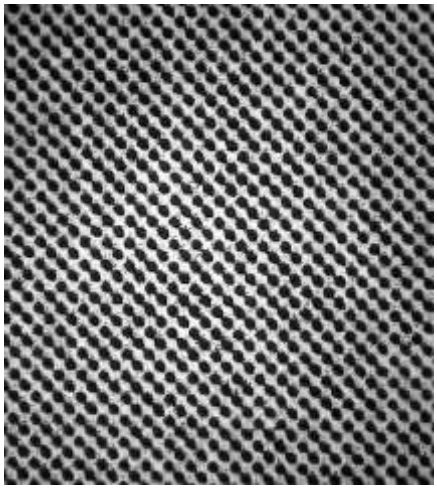

HiROX image of Standard 3

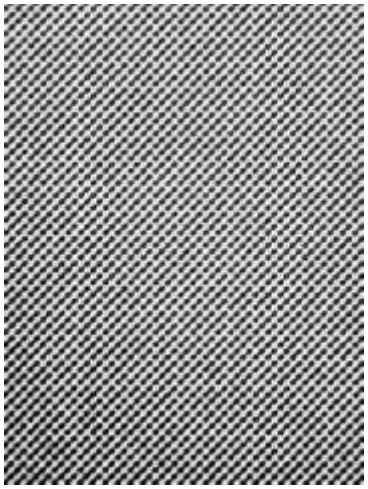

Leica image of Standard 3

REFERENCES

Basu S.K, Deb S.R., and Aggarwal P.S. 1982 Use of Porous Ceramics In Purification of Water. *Glass and Ceramic Bulletin*, 29(2).

Camper A.K., LeChevallier M.W., Broadaway S.C., and McFeters G.A. 1985 Growth and persistence of pathogens on granular activated carbon filters. *Applied and Environmental Microbiology*, 50(6), 1378-1382.

Ceramics Manufacturing Working Group 2011 *Best Practice Recommendations for Local Manufacturing of Ceramic Pot Filters for Household Water Treatment* 1st edn, Center for Disease Control and Prevention, Atlanta, GA, USA.

Clark K.N. and Elmore A.C. 2011 Bacteria removal effectiveness of ceramic pot filters not applied with colloidal silver. *Water Science and Technology: Water Supply*, 11(6), 765-772.

Elmore A.C., Miller G.R., Parker B. 2005 Water quality in Lemoa, Guatemala. *Environmental Geology*, 48, 901-907.

Hubbel L., Elmore A.C., Reidmeyer M. (in press) Comparison of a native clay soil and an engineered clay used in experimental ceramic pot filter fabrication. *Water Science and Technology: Water Supply*.

Hunter P.R. 2009 Household water treatment in developing countries: comparing different intervention types using meta-regression. *Environmental Science and Technology*, 43, 8991-8997.

LeChevallier M.W., Hassenauer T.S., Camper A.K. and McFetters G.A. 1984 Disinfection of bacteria attached to granular activated carbon. *Applied and Environmental Microbiology*, 48(5), 918-923.

Oyandel-Craver V.A. and Smith J.A. 2007 Sustainable colloidal-silver-impregnated ceramic filter for point-of-use water treatment. *Environmental Science and Technology*, 42, 927-933.

Ren D. and Smith J.A. 2013 Retention and transport of silver nanoparticles in a ceramic porous medium used for point-of-use water treatment. *Environmental Science and Technology*, 47, 3825-3832.

Sarikaya A. and Dogan F. 2012 Effect of various pore formers on the microstructural development of tape-cast porous ceramics. *Ceramics International*, 39, 403-413.

Sobsey M.D., Stauber C.E., Casanova L.M., Brown J.M., and Elliott M.A. 2008 Point of use household drinking water filtration: a practical, effective solution for providing

sustained access to safe drinking water in the developing world. *Environmental Science and Technology*, 42, 4261-4267.

Standard Test Methods for Apparent Porosity, Liquid Absorption, Apparent Specific Gravity, and Bulk Density of Refractory Shapes by Vacuum Pressure 2011, C830-00, American Society for Testing and Materials, West Conshohocken, PA, USA.

van Halem D., Heijman S.GJ., Soppe A.I.A., van Dijk J.C. and Amy G.L. 2007 Ceramic silver-impregnated pot filters for household drinking water treatment in developing countries: material characterization and performance study. *Water Science and Technology: Water Supply*, 7(5-6), 9-17.

World Health Organization and United Nations Children's Fund 2014 *Progress on Sanitation and Drinking-water: 2012 Update*. Geneva, Switzerland.

VITA

Jessie Yvonne Hahn was born in Cape Girardeau, Missouri, USA on January 20, 1991. In May 2013 she received her B.S. in Geological Engineering from the Missouri University of Science and Technology, Rolla, Missouri, USA. As an undergraduate student, Jessie dedicated time to the Engineers Without Borders organization focusing on a water supply project in Guatemala. She was also involved with the Missouri University of Science and Technology literary magazine, *Southwinds*. Jessie worked for the United States Army Corps of Engineers in their construction division at Fort Leonard Wood as a student intern during the summers of 2012, 2013, and 2014. She has acted as a Graduate Teaching Assistant for International Engineering and Design, Subsurface Hydrology, and Geomorphology courses in the Geological Engineering program during her time as a graduate student. Jessie received her M.S. Degree in Geological Engineering in May 2015 from the Missouri University of Science and Technology, Rolla, Missouri, USA.

Jessie has been a member of the American Society of Civil Engineers (ASCE) since 2013, a member of the Association of Environmental and Engineering Geologists since 2013, and a member of the Water Environment Federation since 2014.